

# Proteomic analysis of energy metabolism and signal transduction in irradiated melanoma cells

Lu-Bin Yan<sup>1</sup>, Kai Shi<sup>2</sup>, Zhi-Tong Bing<sup>3</sup>, Yi-Lan Sun<sup>2</sup>, Yang Shen<sup>1</sup>

**Foundation item:** The Foundation for Young Talents of Gansu Province, China (No. 1208RJYA013)

<sup>1</sup>Department of Surgery, the Second Hospital of Lanzhou University, Lanzhou 730030, Gansu Province, China

<sup>2</sup>Department of Ophthalmology, the Second Hospital of Lanzhou University, Lanzhou 730030, Gansu Province, China

<sup>3</sup> Institute of Modern Physics, Chinese Academy of Sciences, Lanzhou 730000, Gansu Province, China

**Co-first authors:** Lu-Bin Yan and Kai Shi

**Correspondence to:** Kai Shi. Department of Ophthalmology, the Second Hospital of Lanzhou University, Lanzhou 730030, Gansu Province, China. 1355510989@qq.com

Received: 2012-11-26

Accepted: 2013-05-06

## Abstract

• **AIM:** To analyze proteomic and signal transduction alterations in irradiated melanoma cells.

• **METHODS:** We combined stable isotope labeling with amino acids in cell culture (SILAC) with highly sensitive shotgun tandem mass spectrometry (MS) to create an efficient approach for protein quantification. Protein – protein interaction was used to analyze relationships among proteins.

• **RESULTS:** Energy metabolism protein levels were significantly different in glycolysis and not significantly different in oxidative phosphorylation after irradiation. Conversely, tumor suppressor proteins related to cell growth and development were downregulated, and those related to cell death and cell cycle were upregulated in irradiated cells.

• **CONCLUSION:** Our results indicate that irradiation induces differential expression of the 29 identified proteins closely related to cell survival, cell cycle arrest, and growth inhibition. The data may provide new insights into the pathogenesis of uveal melanoma and guide appropriate radiotherapy.

• **KEYWORDS:** melanoma cell; 2D-LC-MS/MS; stable isotope labeling with amino acids; proteomic analysis; X-ray irradiation; protein-protein interaction

**DOI:**10.3980/j.issn.2222-3959.2013.03.06

energy metabolism and signal transduction in irradiated melanoma cells. *Int J Ophthalmol* 2013;6(3):286–294

## INTRODUCTION

Uveal malignant melanoma is the most frequent primary intraocular neoplasm in adults [1]. Radiotherapy is a highly effective treatment option in cancer management; together with surgery and chemotherapy, it plays an important role in the treatment of 40% of patients who undergo radiotherapy are ultimately cured of their cancer [2]. Although radiotherapy has rapidly developed in recent years, the underlying cellular and molecular mechanisms of radioresistance are not fully understood. Furthermore, high doses of radiation can increase the risk of injury to normal tissues and lead to side effects. Thus, it is imperative to study the sensitivity of uveal melanoma cells to radiotherapy. Although a previous study reported that melanoma cells undergo cell cycle arrest after being exposed to high levels of irradiation, the molecular mechanism is not clear [3]. Furthermore, studying the complicated molecular changes in melanoma cells exposed to ionizing radiation is also challenging [4]. Quantitative proteomic provides a novel way to investigate large numbers of differentially expressed proteins in single experiments. In recent years, liquid chromatography coupled with tandem mass spectrometry (LC-MS/MS) has been increasingly used for proteomic studies because it has the advantages of high throughput and sensitivity, especially when combined with stable isotope labeling with amino acids in cell culture (SILAC) to create an efficient approach for large-scale protein quantification [5-7].

Aerobic glycolysis is generally accepted as a metabolic hallmark of cancer [8], but its relationship with cancer progression after irradiation is still unclear. New insights suggest that it would be useful to target tumor metabolism [9]. Recent research found that aerobic glycolysis would be closely associated with cancer cells survival and growth [10-13]. In addition, tumor progression is characterized by alterations in cell signaling [14]. With MS technologies and bioinformatics tools, it is possible to track and analyze signaling events in irradiated cancer cells. Recent research has shown that many signaling proteins regulate cancer cell growth and metabolism, including RAC-alpha serine/threonine-specific protein kinase (Akt), mammalian target of rapamycin (mTOR), cellular tumor antigen p53 (TP53), and others [15-17].

Furthermore, mapping signaling and metabolism protein interactions might help identify the molecular mechanisms at work in irradiated melanoma cells. Indeed, many studies have reported that energy metabolism is closely associated with radioresistance and radiosensitivity<sup>[18, 19]</sup>.

In this study, we applied SILAC technology coupled with 2D-LC-MS/MS and quantitative proteome and interaction network analysis to elucidate metabolism and signaling pathways in irradiated melanoma cells. The quantitative proteomics data described here provide new insights into novel targets for radiotherapy.

## MATERIALS AND METHODS

### Materials

**Cell culture** Human choroidal malignant melanoma cell line 92-1 was kindly provided by Modern Physics researchers at the Chinese Academy of Science. All cells were kept in a humidified atmosphere of 95% air and 5% CO<sub>2</sub> at 37°C, and 5×10<sup>5</sup> cells were seeded in 25cm<sup>2</sup> culture flasks 2 days before irradiation, which resulted in <70% confluence at the time of irradiation. For SILAC experiments, the 15 hours post-irradiation group cells were cultured in heavy Dulbecco's modified essential medium (DMEM) containing L-arginine-<sup>13</sup>C<sub>6</sub><sup>15</sup>N<sub>4</sub>, and control cells were maintained in light L-arginine-<sup>12</sup>C<sub>6</sub><sup>14</sup>N<sub>4</sub> medium.

**Irradiation** After 48 hours normal incubation, cells were irradiated at room temperature using a Pantak-320S generator (Shimadzu, Tokyo, Japan) operated at 200kVp and 20mA with 0.5-mm Al and 0.5-mm Cu filters at a dose of 10Gy and were then cultured for 15 hours. The dose rate was 1Gy/min. After 15 hours further culture, SILAC cells were washed three times with ice-cold (0-4°C) phosphate-buffered saline (PBS) separately for extraction.

**Sample preparation** Cells were scraped into 8mol/L urea and sonicated at 4°C to lyse the cells. After centrifugation for 30 minutes at 20 000×g, the supernatants were collected and kept at -80°C until analysis. Protein concentrations were measured using the Bradford method. Extracted protein samples from heavy and light serum were combined at a 1:1 ratio. The samples were dissolved in 8mmol/L urea and 25mmol/L NH<sub>4</sub>HCO<sub>3</sub> and reduced with 10mmol/L DTT for 1 hour at room temperature. Samples were alkylated by 40mmol/L iodacetamide in the dark for 1 hour at room temperature, and then 40mmol/L DTT was added to quench the iodacetamide for 1 hour at room temperature. After diluting 8mol/L urea with 25mmol/L NH<sub>4</sub>HCO<sub>3</sub> to 0.6mol/L, trypsin was added at a ratio of 1:40 and digested at 37°C overnight. In order to completely cleave the proteins, trypsin was added to the sample at a ratio of 1:40 again and digested at 37°C for 8 hours. Finally, trypsin digestion was stopped by adding formic acid (FA) for a 1% final concentration.

### Methods

**2D-LC-MS/MS analysis** The samples were analyzed by

two-dimensional liquid chromatography (2D-LC) on an LTQ mass spectrometer (Thermo Fisher Scientific, Waltham, MA, USA) according to a previously published method<sup>[20]</sup>. The tryptic peptide mixtures were analyzed by 2D-LC coupled to a linear ion trap mass spectrometer LTQ (ThermoElectron, Waltham, MA, USA). For each experiment, the peptide mixtures (from about 100µg proteins) were pressure-loaded onto a biphasic silica capillary column (250µm inner diameter [i.d.]) packed with 3cm reverse-phase C18 resin (SP-120-3-ODS-A, 3mm, the Great Eur-Asia Sci&Tech Development, Beijing, China) and 3cm strong cation exchange resin (Luma 5µm SCX 100A, Phenomenex, Torrance, CA, USA). The buffers used were 0.1% FA (buffer A), 80% acetonitrile (ACN)/0.1% FA (buffer B), and 600mmol/L ammonium acetate/5% ACN/0.1% FA (buffer C). After sample loading, the biphasic column was first desalted with buffer A and then eluted using a 10-step salt gradient ranging from 0 to 600mmol/L ammonium acetate. After each salt gradient, a gradient of buffer B ranging from 0 to 100% was applied. Step 1 consisted of a 100-minute gradient from 0 to 100% buffer B. For steps 2-9, after equilibrating with buffer A for the first 3 minutes, X% buffer C was applied for 5 minutes, and peptides were eluted using a linear gradient as follows: 0%-10% buffer B in 5 minutes, 10%-45% buffer B in 77 minutes, 45%-100% buffer B in 10 minutes, and 100% buffer B for 10 minutes, followed by re-equilibration with buffer A for 10 minutes. The 5-minute buffer C percentages (X) were 5%, 10%, 15%, 20%, 25%, 35%, 50%, and 75%. The gradient used in the final step contained 3 minutes of 100% buffer A, 20 minutes of 100% buffer C, a 5-minute gradient from 0% to 10% buffer B, a 72-minute gradient from 10% to 55% buffer B, and a 5-minute gradient from 55% to 100% buffer B. Then, 100% buffer B was applied for 5 minutes, followed by a 5-minute elution with buffer A and another 10-minute elution with buffer B. The effluent of the biphasic column in each case was directed into an in-house-packed 10-cm C18 analytical column (100µm i.d., SP-120-3-ODS-A, 3mm) with a 3- to 5-µm spray tip. The flow rate at the tip was maintained at about 500nL/min. Nano-electrospray ionization was performed at a spray voltage of 1.9kV and a heated capillary temperature of 170°C. The MS instrument was set to the data-dependent acquisition mode with dynamic exclusion turned on, and maximum ion injection time was set to 100ms. One MS survey scan, with mass range 400-2000m/z, was followed by five MS/MS scans. All tandem mass spectra were collected using a normalized collision energy (35% setting), an isolation window of 2Da, and 1 micro-scan. The XCalibur data system (ThermoElectron, Waltham, MA, USA) was used to control the high-performance liquid chromatographic (HPLC) solvent gradients and apply the MS scanning functions. MS data were searched using SEQUEST

algorithm (Ver. 2.8) against the human database, which was released on May 27, 2008, and contains 37 869 protein sequences. The database was reversed and attached to estimate the false discovery rate (FDR).

**Western blot analysis** An antibody against lactate dehydrogenase B (LDHB) (sc-100775) was purchased from Santa Cruz Biotechnology (Santa Cruz, CA, USA). Cells were collected and lysed in appropriate amounts of lysis buffer (Biyuntian, Nanjing, China). The samples were mixed with sample buffer (250mmol/L Tris HCl, 5%  $\beta$ -mercaptoethanol, 50% glycerol, 10% sodium dodecyl sulfate [SDS], and 0.5% bromophenol blue) and boiled for 5 minutes, and equal amounts of protein (30 $\mu$ g) were separated on 10% SDS-polyacrylamide gels (Bio-Rad, Hercules, CA, USA). Blotting was performed at 120V for 1.5 hours in a wet transfer instrument (Bio-Rad). The membranes were then washed three times with PBS containing 0.1% Tween-20 and incubated with secondary antibody for 1 hour. Finally, the membrane was washed, protein bands were visualized using an enhanced chemiluminescence system (Amersham-Buchler, Braunschweig, Germany), and the membranes were exposed to X-ray medical film (Kodak, Rochester, NY, USA).

**Cell cycle assay** The cells were incubated for several different phases post-irradiation before they were collected and fixed for 24 hours at -20°C with 70% ethanol. The fixed cells were washed with PBS, treated with 100 $\mu$ g/mL RNase A and 50 $\mu$ g/mL propidium iodide for 30 minutes. Cell cycle distribution was analyzed with Modfit software (Verity Software, Topsham, ME, USA) from the histogram of DNA content measured with a flow cytometer (FACSan, Becton Dickinson, Franklin Lakes, NJ, USA).

**Cell proliferation assay** Exponentially growing cells were seeded on sterile cover slips at a density of  $1 \times 10^5$ /well, incubated for 48 hours later, irradiated with X-rays, fixed in 4% paraformaldehyde for 10 minutes and in methanol at -20°C for 5 minutes, permeabilized with 0.5% Triton X-100 for 1 hour, blocked in buffer (5% skim milk with 0.5% Triton X-100) for 2 hours, and stained with a primary Ki67 antibody at 1:50 dilution (Cell Signaling Technology, Danvers, MA, USA) for 2 hours. The bound antibody was visualized using Alexa Fluor 594 anti-rabbit antibody (Molecular Probes, Eugene, OR, USA), and cell nuclei were counterstained with DAPI (4',6-diamidino-2-phenylindole) solution (Invitrogen, Carlsbad, CA, USA). Photos were taken with a fluorescent microscope (Keyence, Tokyo, Japan). Ki67-positive cells were counted by using a fluorescent microscope, and at least 500 cells were scored for each sample.

**Glycolysis production measurements** Lactate production was measured using an enzymatic kit (Nanjing, Jiancheng, China) according to the manufacturer's instruction. The results were normalized by cell counts. Briefly, NAD<sup>+</sup> was

added to media and stoichiometrically converted to NADH by lactate in the media. The levels of NADH were then colorimetrically quantified.

**Data analysis and bioinformatics** Resulting data were collected using Xcalibur and interpreted by SEQUEST of Bioworks 3.3.1 (Thermo Fisher Scientific) using the NCBI database. Bioworks was used to analyze and filter peptide identifications, *i.e.*, Xcorr  $\geq 1.8$  ( $z=1$ ), 2.2 ( $z=2$ ), 3.5 ( $z=3$ ), Sp  $\geq 500$ , Rsp  $\geq 5$ , proteins with Number of peptide  $\geq 2$ , and Consensus score  $\geq 10$ . Subsequent analysis included assigning peptides to the spectra, validating the peptide assignments to remove incorrect results, determining relative quantitation ratios between heavy and light isotopic labeling, and inferring protein identifications from the assigned peptides. An open source tool called TPP (Version 4.4.1) could perform these steps: PeptideProphet validates peptides assigned to MS/MS spectra<sup>[21]</sup>, XPRESS program quantitate peptides<sup>[22]</sup> and proteins in differentially labeled samples, and ProteinProphet<sup>[23]</sup> infers sample proteins. In addition, the minimum peptide length was considered as seven, and results below the PeptideProphet probability at 0.95 were filtered out. The annotations and biologic processes of proteins were obtained from the Human Protein Reference Database (HPRD Version 04-13-10, <http://www.hprd.org>). For proteins without descriptions, annotations were identified by searching the UniProt and National Center for Biotechnology Information (NCBI) protein databases. This study classified proteins according to go ontology (GO) biology processes from the HPRD database. Proteins were considered to be significantly dysregulated if the fold change in protein expression between sham and irradiated samples was  $\geq \pm 1.50$  and  $P \leq 0.05$  ( $t$ -test).

**Protein-protein interaction network analysis** The identified proteins were mapped to networks available in the STRING 9.0 database (<http://string-db.org/>) and displayed by Cytoscape 2.8.1 (<http://www.cytoscape.org/>). In this study, Ingenuity Pathway Analysis (IPA Ingenuity® Systems, [www.ingenuity.com](http://www.ingenuity.com)) was applied to obtain information regarding the relationships, biological mechanisms, functions, and pathways of differentially regulated proteins. The fold change with log<sub>2</sub> ratio and IPI accession number of dysregulated proteins were submitted to IPA.

**Statistical Analysis** Statistical analysis was performed using Statistical Product and Service Solutions (SPSS13.0). The band densities were quantified as fold-change using Student's  $t$ -tests based on the mean of three replicates.  $P$  value of 0.05 or less was considered significant.

## RESULTS

**Identification and quantification of dysregulated proteins** The simple LC-MS/MS workflow is depicted in Figure 1. In the filtered results, 189 proteins involved in cell communication and signal transduction (CC and ST) and

**Table 1 Proteins with largest increased and decreased expression in melanoma cells post-irradiation for 15 hours**

Proteins	Refseq	Gene name	Xpress ratio	Unique peptides	Coverage (%)	Description	Biological process
Ten proteins with largest increase in expression in melanoma cells	NP_002291.1	LDHB	11.11±0.04	13	47.3	lactate dehydrogenase B	Metabolism (GO:0008152); Energy pathways (GO:0006091)
	NP_000131.2	FECH	4.55±0.00	1	1.9	ferrochelatase isoform b precursor	Metabolism (GO:0008152); Energy pathways (GO:0006091)
	NP_006089.1	GNB2L1	2.86±0.25	6	19.6	guanine nucleotide binding protein (G protein) tumor necrosis factor receptor 1 precursor	Cell communication (GO:0007154); Signal transduction (GO:0007165)
	NP_001056.1	TNFRSF1A	2.86±0.00	1	3.3	acetyl-Coenzyme A acetyltransferase 1	Cell communication (GO:0007154); Signal transduction (GO:0007165)
	NP_000010.1	ACAT1	2.86±0.00	1	1.9	hexokinase 1	Metabolism (GO:0008152); Energy pathways (GO:0006091)
	NP_277031.1	HK1	2.33±0.05	3	4.2	Macrophage migration inhibitory factor	Metabolism (GO:0008152); Energy pathways (GO:0006091)
	NP_002406.1	MIF	2.13±0.13	5	46.1	peroxisomal enoyl-coenzyme A hydratase-like protein	Cell communication (GO:0007154); Signal transduction (GO:0007165)
	NP_001389.2	ECH1	0.25±0.00	1	4.9	adenylate kinase 2 isoform	Metabolism (GO:0008152); Energy pathways (GO:0006091)
	NP_001616.1	AK2	0.26±0.04	2	7.3	peroxiredoxin 1	Metabolism (GO:0008152); Energy pathways (GO:0006091)
	NP_859047.1	PRDX1	0.36±0.63	8	22.6	peroxiredoxin 3	Cell communication (GO:0007154); Signal transduction (GO:0007165)
Ten proteins with largest decrease in expression in melanoma cells	NP_054817.2	PRDX3	0.37±1.21	3	15.5	casein kinase 2	Cell communication (GO:0007154); Signal transduction (GO:0007165)
	NP_001887.1	CSNK2A2	0.37±0.00	1	5.7	glucosamine-fructose-6-phosphate aminotransferase	Cell communication (GO:0007154); Signal transduction (GO:0007165)
	NP_002047.1	GFPT2	0.38±0.00	1	1.5	breakpoint cluster region isoform 1	Metabolism (GO:0008152); Energy pathways (GO:0006091)
	NP_004318.3	BCR	0.38±0.00	1	3.2	dihydropyrimidinase-like 2	Cell communication (GO:0007154); Signal transduction (GO:0007165)
	NP_001377.1	DPYSL2	0.41±0.09	5	8.4	orexin precursor	Cell communication (GO:0007154); Signal transduction (GO:0007165)
	NP_001515.1	HCRT	0.42±0.00	1	10.7	tubby like protein 1	Cell communication (GO:0007154); Signal transduction (GO:0007165)
	NP_003313.3	TULP1	0.43±0.00	1	3.5		Cell communication (GO:0007154); Signal transduction

metabolism and energy pathways (M and EP) were identified, among which 19 proteins were upregulated, 29 were downregulated, and 141 were unchanged. These proteins were sorted by GO from the HPRD Database. LDHB was identified by 13 unique peptides, and the coverage ratio was 47.3% (Supplementary File). In Table 1, we listed the 10 proteins with the largest increase in expression levels and the 10 proteins with the largest decrease. Less dysregulated proteins are listed in Supplementary file 3 and were mainly involved in metabolism processes. For example, proteins such as SOD3, GSS, and ST13 have oxidative reduction functions, suggesting that the cells were under oxidative stress. Some slightly upregulated proteins, such as ATP5O, COX6A1, and HADHA, were mitochondrial and involved in ATP production. Other minor upregulated proteins such as NANS, CNP, and GNPDA1 were mainly involved in glycolysis and nucleotide metabolism, indicating that the cells maintained high metabolism levels to combat the stress of radiation.

**Western blotting analysis** LDHB and PFKM proteins were selected to verify MS data. The SILAC ratios of LDHB and PFKM showed dramatic up- and downregulation post-irradiation with 10-Gy X-rays, respectively (Figure 2). The expression changes of LDHB and PFKM were confirmed by Western blot analysis, which showed that changes were basically identical with SILAC (Table 2).

**Phenotype assessments** We performed cell cycle assays and found that irradiated cells were subject to cell cycle arrest (Figure 3A), similar to as reported in previous studies [3]. The lactate production level was used to investigate glycolysis

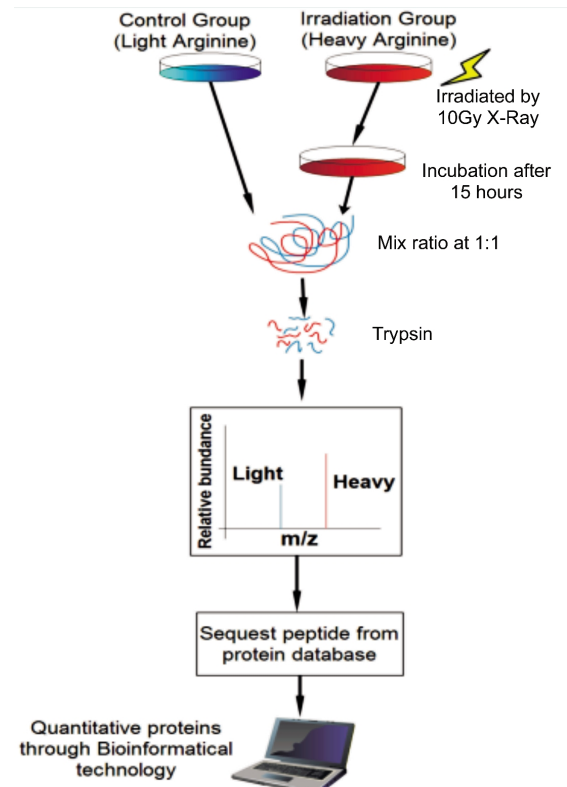


**Figure 1 A simple workflow of quantitative shotgun proteomics.**

**Table 2 Comparison of SILAC ratio and Western blot quantitation**

Gene name	SILAC ratio	Normalized ratio
LDHB	11.11±0.04	2.48±0.23
PFKM	0.55±0.06	0.74±0.05

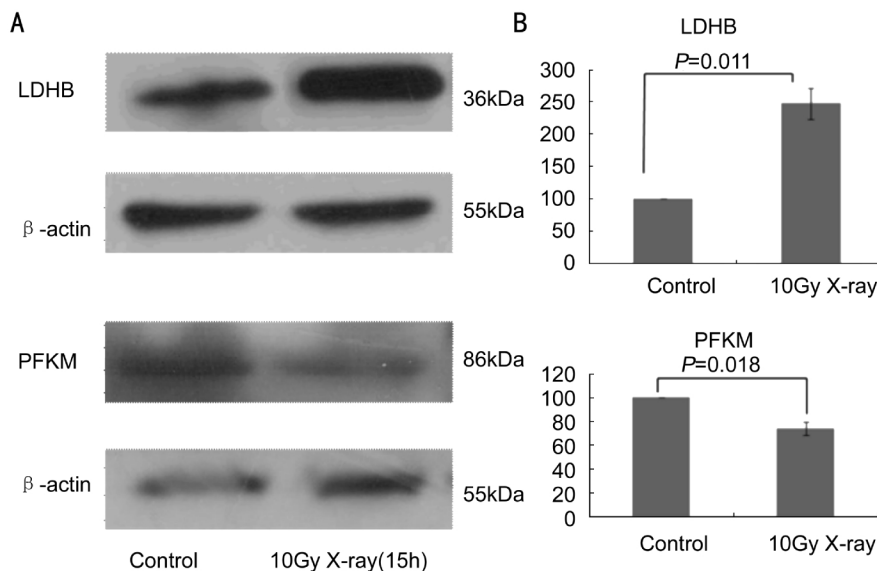


**Figure 2 Western blot analysis of LDHB** A: Western blot analysis showing expression level changes of LDHB and PFKM at 15- and 48-hour post-irradiation in 92-1 cells; B: Histograms represent the average±SEM of LDHB and PFKM protein levels relative to β-actin levels in each group.

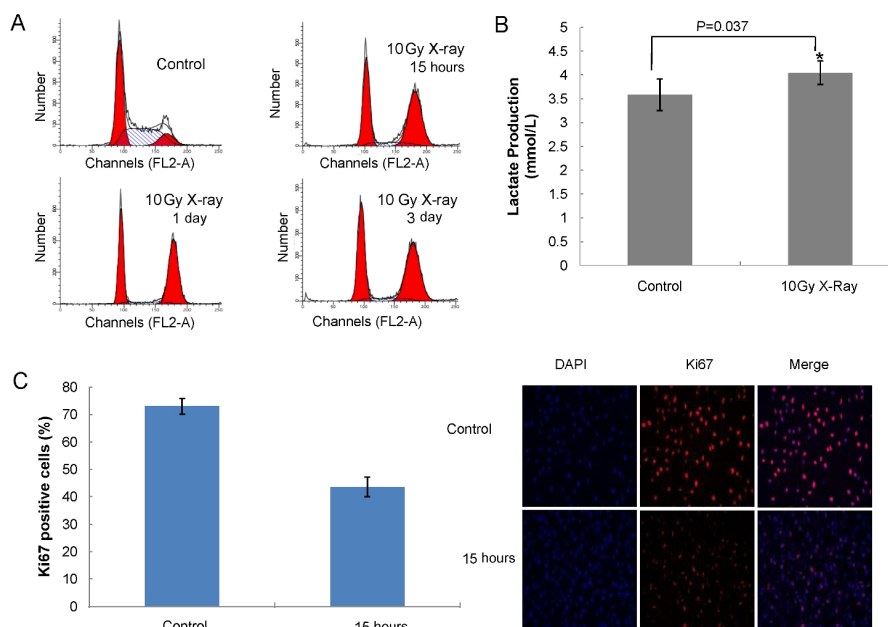


**Figure 3 Post-irradiation cell phenotypes** A: FACS cell cycle analysis; B: Lactate production at 15-hour post-irradiation; C: Ki67 immunofluorescent staining quantitation (left) and representative images (right).

alterations. The lactate generated at the end of the glycolysis pathway and the level of lactate production would reflect the glycolysis flux. Figure 3B shows that the level of lactate production was significantly higher post-irradiation, indicating that cells increased glycolysis in response to irradiation. Cell proliferation post-irradiation was another area of interest in this study. Ki67 is a widely accepted marker for determining cell proliferation [24]. As shown in Figure 3C, Ki67 immunoreactivity was significantly decreased post-irradiation, which indicated that radiation inhibited proliferation.

**Changes in energy pathway protein levels induced by irradiation** We assessed changes in energy pathway protein

levels in melanoma cells 92-1 after irradiation. Differentially expressed proteins in response to 10-Gy X-Ray irradiation are depicted in Figure 4. Energy pathways are separated into four types by dashed lines. (glycolysis, TCA cycle, oxidative phosphorylation, and pantose phosphate pathway). Expression fold change  $\geq 1.5$  or  $\leq 0.67$  was considered significant [25]. Previous research demonstrated that cell cycle arrest in 92-1 melanoma cells is induced by irradiation with 10Gy for 15 hours [3]. HK1, LDHB, COX6A1, and ATP5O were significantly increased and PFKM, TKT, and NDUFB10 were significantly decreased.

**Irradiation-induced changes in signal transduction protein levels** ST proteins that regulate metabolism were

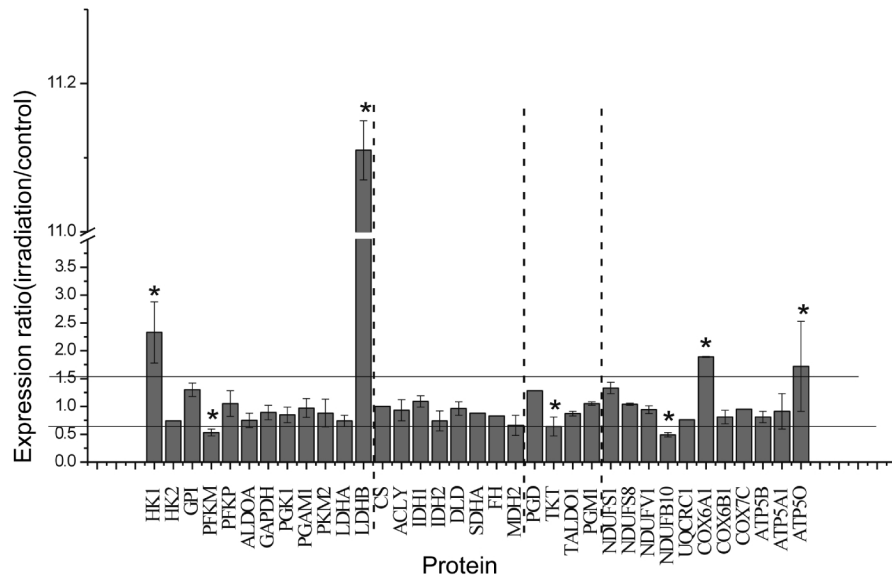


**Figure 4 Relative quantification of the energy pathway proteome in response to 10-Gy X-ray treatment of 92-1 melanoma cells**  
 The energy pathway was separated into four sections by dashed line, to divide the glycolysis, TCA cycle, oxidative phosphorylation and pantose phosphate pathways. Bars above the top horizontal line represent significantly increased proteins. Bars lower than bottom horizontal line represent significantly decreased proteins.

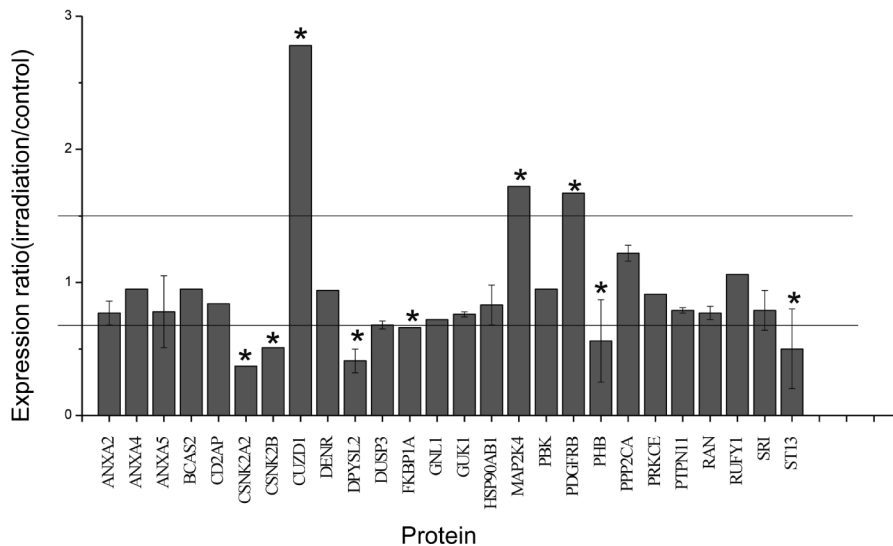


**Figure 5 Relative quantification of signal transduction proteins involved in metabolism in response to 10-Gy X-ray treatment of 92-1 melanoma cells**  
 Bars above the top horizontal line represent significantly increased proteins. Bars lower than bottom horizontal line represent significantly decreased proteins.

sorted by the PANTHER Classification system (<http://www.pantherdb.org/>). Their relative quantifications are shown in Figure 5. CUZD1, MAP2K4, and PDGFRB were upregulated. MAP2K4 is a tumor suppressor in many cancer cells and is a component of a stress and cytokine-induced signaling pathway involving MAPK proteins [26,27]. PDGFRB is considered as a cytoplasmic ATM activator that protects some cells from oxidative stress[28].

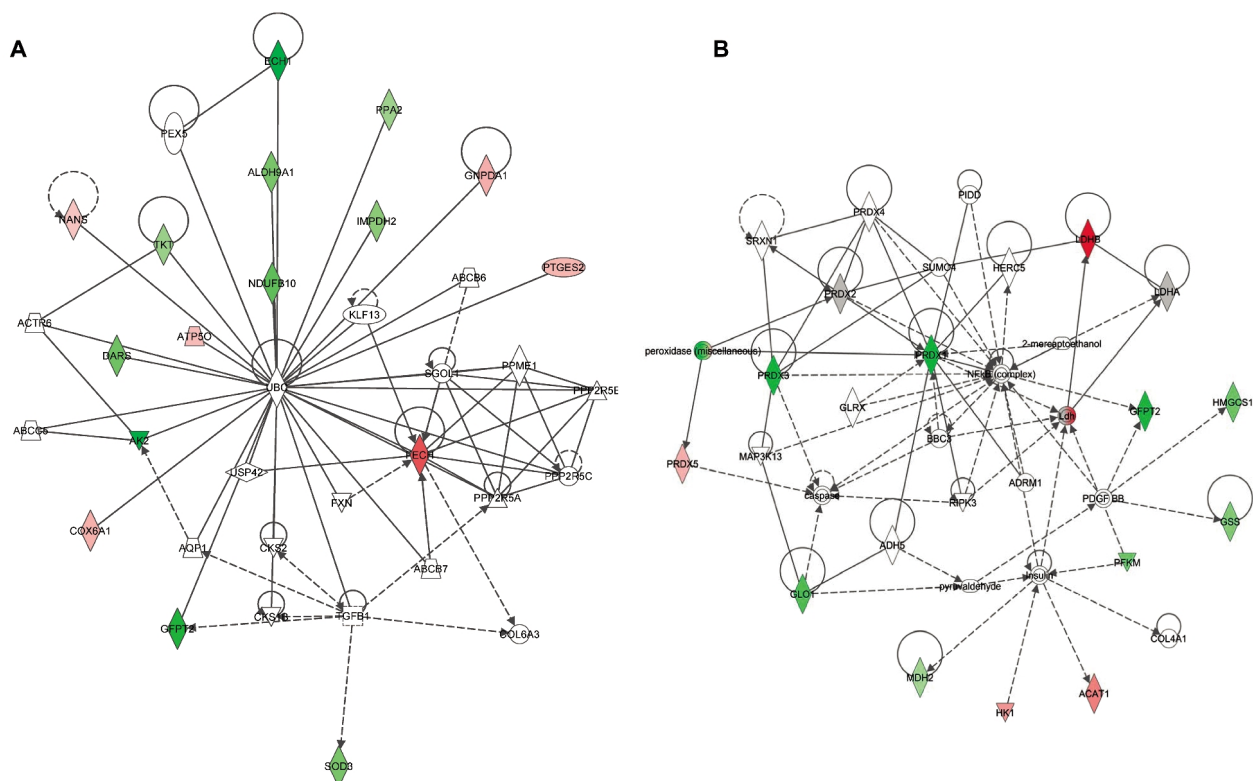
**Post-irradiation protein network analysis of metabolism and signaling transduction pathways** To further understand cell regulation post-irradiation, IPA was applied to analyze the protein networks of metabolic and signaling transduction processes. For metabolic processes, we found two networks with significant scores, and these are shown in

Figure 6. One was "Molecular Transport, Small Molecular Biochemistry, and Cell Cycle," with a highly significant score of 40 (Figure 6A), and the second was "Free Radical Scavenging, Small Molecule Biochemistry, Protein Synthesis, " with a score of 28 (Figure 6B).

For signaling transduction, the most significantly dysregulated network was "Cell Death and Survival, Cell Cycle, and Post-Translational Modification," with a score of 42 (Figure 7).

**DISCUSSION**

Our analysis employs targeted proteomics to study metabolism and signal transduction in melanoma cells. Glycolysis-related proteins are elevated in most cancer cells according to the "Warburg effect" [29]. We found that HK1



**Figure 6 Schematic representation of proteins associated with metabolism networks using IPA** A: The network "Molecular Transport, Small Molecule Biochemistry, and Cell Cycle" had a highly significant score of 40; B: The network "Free Radical Scavenging, Small Molecule Biochemistry, Protein Synthesis" had a highly significant score of 28. Green and red colors indicate proteins found to be downregulated and upregulated in our study, respectively.

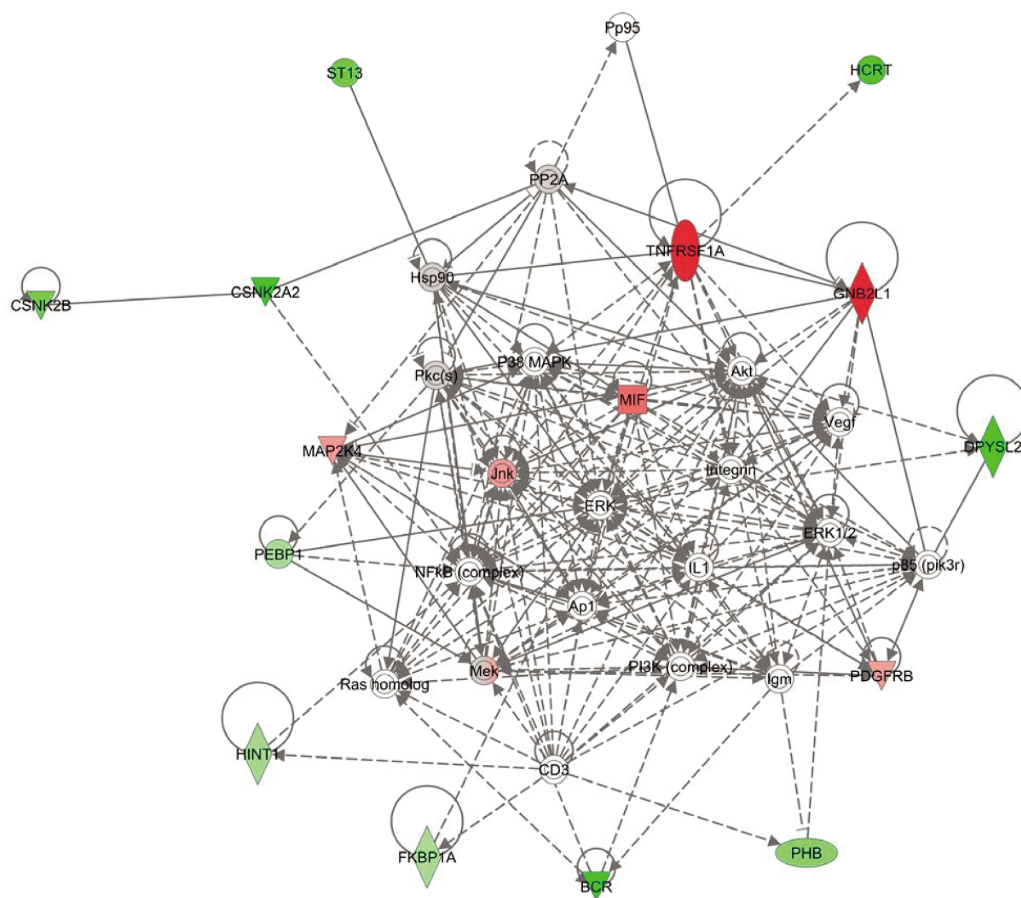


**Figure 7 Schematic representation of proteins associated with signal transduction networks using IPA** The network "Cell Death and Survival, Cell Cycle, and Post-Translational Modification" had a highly significant score of 42. Green and red colors indicate proteins found to be downregulated and upregulated in our study, respectively.

and LDHB were upregulated and PFKM was downregulated. Previous studies reported that HK2, LDHA, and PFKM were direct targets of *Myc* [30-32]. However, the significance of LDHB in tumor development remains elusive, and the regulation of its expression is also less characterized. However, recent studies show that mTOR is a positive regulator of LDHB [33]. HK1 is considered as the first step in glycolysis and is a likely candidate for the control of glucose metabolism [34]. Generally, HK1 expression increase was indicative of previous glucose uptake. Recent evidence suggests that HK1 may also have an antiapoptotic role [35]. Indeed, previous experiments showed that irradiated cells do not undergo apoptosis [3].

CSNK2A2, CSNK2B, DPYSL2, FKBP1A, PHB, and ST13 were downregulated 15 hours after irradiation CSNK2A2 and CSNK2B are catalytic and regulatory subunits of the protein complex CKII (casein kinase II), respectively. CKII plays an important role in cell cycle progression, and CKII-inactivated cells may arrest in G<sub>1</sub> due to upregulation of Sic1 (cyclin-dependent kinase inhibitor) [36, 37]. Previous research indicated that p53 may lose the ability to maintain mitotic integrity in CKII absence or dysfunction via a loss of its ability to appropriately regulate cyclin B levels, as well as an inability to execute apoptosis [38]. CSNK2B/CK2 $\beta$  is a regulatory subunit of CKII, which is considered as a vital protein that regulates cell cycle in both G<sub>1</sub> and G<sub>2</sub>/M phases. Yde *et al* [39] found that downregulating CK2 $\beta$  by RNA interference resulted in delayed cell cycle progression at the onset of mitosis.

PHB and ST13 are considered to be tumor suppressor proteins [40, 41]. PHB binds to Rb proteins and represses E2F transcriptional activity. The mechanism by which DPYSL2, FKBP1A, PHB, and ST13 are downregulated following irradiation remains unclear.

Based on the cell phenotypes observed post-irradiation (Figure 3), we inferred that the antiapoptosis pathways might be closely associated with glycolysis enhancement and other key proteins involved in signal transduction.

For metabolic processes, we found that the second network included many key proteins (Figure 6B). Recent research has shown that GLO1 is upregulated in various human malignant tumors, including melanoma [42,43]. Moreover, GLO1 overexpression has been associated with cancer cell survival and resistance to chemotherapeutic agents [44]. We found that GLO1 was significantly downregulated, and cell cycle arrest was observed at 15 hours. Moreover, antioxidant enzymes including PRDX1, PRDX2, and PRDX3 were also downregulated, although PRDX5 was not. Besides its role as an antioxidant, the effects of PRDX5 upregulation after radiation remain unknown. We inferred that attenuating antioxidant functions in irradiated melanoma cells might

induce more serious DNA damage.

With regard to signaling transduction processes, the affected network was closely associated with cell survival and cell cycle. Some important regulators, such as NF- $\kappa$  B complex, PI3K/Akt, and MAPK/Jnk might play vital roles in cell cycle arrest and cell survival [45-47]. One limitation of this 2D-LC/MS/MS study is that it was difficult to detect regulator proteins due to their low levels.

In summary, we demonstrated changes in metabolism and signal transduction protein pathways in irradiated melanoma 92-1 cells with SILAC and 2D-LC-MS/MS. We set out to investigate mechanisms of cell cycle arrest, antiapoptosis, and growth inhibition following irradiation and identified several key regulatory proteins in cell cycle and cell survival. We hope that these findings will be useful in finding regulators that can be targeted to improve uveal melanoma radiotherapy.

#### REFERENCES

- 1 Lopez-Velasco R, Morilla-Grasa A, Saornil-Alvarez MA, Ordonez JL, Blanco G, Rabano G, Fernandez N, Almaraz A. Efficacy of five human melanocytic cell lines in experimental rabbit choroidal melanoma. *Melanoma Res* 2005;15(1):29-37
- 2 Shafiq J, Barton M, Noble D, Lemer C, Donaldson LJ. An international review of patient safety measures in radiotherapy practice. *Radiother Oncol* 2009;92(1):15-21
- 3 He JP, Li JH, Ye CY, Zhou LB, Zhu JY, Wang JF, Mizota A, Furusawa Y, Zhou GM. Cell cycle suspension: a novel process lurking in G<sub>2</sub> arrest. *Cell Cycle* 2011;10(9):1468-1476
- 4 Chen EI, Yates JR. Cancer proteomics by quantitative shotgun proteomics. *Mol Oncol* 2007;1(2):144-159
- 5 Ong SE, Mann M. Mass spectrometry-based proteomics turns quantitative. *Nat Chem Biol* 2005;1(5):252-262
- 6 Ong SE, Blagoev B, Kratchmarova I, Kristensen DB, Steen H, Pandey A, Mann M. Stable isotope labeling by amino acids in cell culture, SILAC, as a simple and accurate approach to expression proteomics. *Mol Cell Proteomics* 2002;1(5):376-386
- 7 Mann M. Functional and quantitative proteomics using SILAC. *Nat Rev Mol Cell Bio* 2006;7(12):952-958
- 8 Hanahan D, Weinberg Robert A. Hallmarks of cancer: the next generation. *Cell* 2011;144(5):646-674
- 9 Pan JG, Mak TW. Metabolic Targeting as an anticancer strategy: dawn of a new era? *Sci STKE* 2007;2007(381):pe14
- 10 Christofk HR, Vander Heiden MG, Harris MH, Ramanathan A, Gerszten RE, Wei R, Fleming MD, Schreiber SL, Cantley LC. The M2 splice isoform of pyruvate kinase is important for cancer metabolism and tumour growth. *Nature* 2008;452(7184):230-U74
- 11 Pitroda SP, Wakim BT, Sood RF, Beveridge MG, Beckett MA, MacDermid DM, Weichselbaum RR, Khodarev NN. STAT1-dependent expression of energy metabolic pathways links tumour growth and radioresistance to the Warburg effect. *BMC Med* 2009;7:68
- 12 Fantin VR, St-Pierre J, Leder P. Attenuation of LDH-A expression uncovers a link between glycolysis, mitochondrial physiology, and tumor maintenance. *Cancer Cell* 2006;9(6):425-434
- 13 Pelicano H, Martin DS, Xu RH, Huang P. Glycolysis inhibition for anticancer treatment. *Oncogene* 2006;25(34):4633-4646

- 14 Irish JM, Kotecha N, Nolan GP. Mapping normal and cancer cell signalling networks: towards single-cell proteomics. *Nat Rev Cancer* 2006; 6(2):146–155
- 15 Gonzalez E, McGraw TE. The Akt kinases: isoform specificity in metabolism and cancer. *Cell Cycle* 2009;8(16):2502–2508
- 16 Robey RB, Hay N. Akt, hexokinase, mTOR: Targeting cellular energy metabolism for cancer therapy. *Drug Discov Today* 2005;2(2):239–246
- 17 Vousden KH, Ryan KM. p53 and metabolism. *Nat Rev Cancer* 2009;9(10):691–700
- 18 Sattler UGA, Meyer SS, Quennet V, Hoerner C, Knoerzer H, Fabian C, Yaromina A, Zips D, Walenta S, Baumann M, Mueller-Klieser W. Glycolytic metabolism and tumour response to fractionated irradiation. *Radiother Oncol* 2010;94(1):102–109
- 19 Pogosova-Agadjanian EL, Fan W, Georges GE, Schwartz JL, Kepler CM, Lee H, Suchanek AL, Cronk MR, Brumbaugh A, Engel JH, Yukawa M, Zhao LP, Heimfeld S, Stirewalt DL. Identification of radiation-induced expression changes in nonimmortalized human T cells. *Radiat Res* 2010; 175(2):172–184
- 20 Cui ZY, Chen XL, Lu BW, Park SK, Xu T, Xie ZS, Xue P, Hou JJ, Hang HY, Yates JR, Yang FQ. Preliminary quantitative profile of differential protein expression between rat L6 myoblasts and myotubes by stable isotope labeling with amino acids in cell culture. *Proteomics* 2009;9(5): 1274–1292
- 21 Keller A, Eng J, Zhang N, Li XJ, Aebersold R. A uniform proteomics MS/MS analysis platform utilizing open XML file formats. *Mol Syst Biol* 2005;1
- 22 Han DK, Eng J, Zhou HL, Aebersold R. Quantitative profiling of differentiation-induced microsomal proteins using isotope-coded affinity tags and mass spectrometry. *Nat Biotechnol* 2001;19(10):946–951
- 23 Nesvizhskii AI, Keller A, Kolker E, Aebersold R. A statistical model for identifying proteins by tandem mass spectrometry. *Anal Chem* 2003;75(17):4646–4658
- 24 Nam HJ, Kim S, Lee MW, Lee BS, Hara T, Saya H, Cho H, Lee JH. The ERK-RSK1 activation by growth factors at G2 phase delays cell cycle progression and reduces mitotic aberrations. *Cell Signal* 2008;20(7): 1349–1358
- 25 Xiong L, Wang Y. Quantitative proteomic analysis reveals the perturbation of multiple cellular pathways in HL-60 Cells Induced by arsenite treatment. *J Proteome Res* 2010;9(2):1129–1137
- 26 Song L, Li J, Zhang D, Liu ZG, Ye J, Zhan Q, Shen HM, Whiteman M, Huang C. IKKbeta programs to turn on the GADD45alpha-MKK4-JNK apoptotic cascade specifically via p50 NF-kappaB in arsenite response. *J Cell Biol* 2006;175(4):607–617
- 27 Spillman MA, Lacy J, Murphy SK, Whitaker RS, Grace L, Teaberry V, Marks JR, Berchuck A. Regulation of the metastasis suppressor gene MKK4 in ovarian cancer. *Gynecol Oncol* 2007;105(2):312–320
- 28 Kim TS, Kawaguchi M, Suzuki M, Jung CG, Asai K, Shibamoto Y, Lavin MF, Khanna KK, Miura Y. The ZFH3 (ATBF1) transcription factor induces PDGFRB, which activates ATM in the cytoplasm to protect cerebellar neurons from oxidative stress. *Dis Model Mech* 2010;3(11–12): 752–762
- 29 Warburg O. On the origin of cancer cells. *Science* 1956;123(3191): 309–314
- 30 Collier HA, Grandori C, Tamayo P, Colbert T, Lander ES, Eisenman RN, Golub TR. Expression analysis with oligonucleotide microarrays reveals that MYC regulates genes involved in growth, cell cycle, signaling, and adhesion. *Proc Natl Acad Sci U S A* 2000;97(7):3260–3265
- 31 O'Connell BC, Cheung AF, Simkevich CP, Tam W, Ren X, Mateyuk MK, Sedivy JM. A large scale genetic analysis of c-Myc-regulated gene expression patterns. *J Biol Chem* 2003;278(14):12563–12573
- 32 Schuhmacher M, Kohlhuber F, Hölzel M, Kaiser C, Burtscher H, Jarsch M, Bornkamm GW, Laux G, Polack A, Weidle UH, Eick D. The transcriptional program of a human B cell line in response to Myc. *Nucleic Acids Res* 2001;29(2):397–406
- 33 Zha X, Wang F, Wang Y, He S, Jing Y, Wu X, Zhang H. Lactate dehydrogenase B is Critical for hyperactive mTOR-mediated tumorigenesis. *Cancer Res* 2011;71(1):13–18
- 34 Paré G, Chasman DI, Parker AN, Nathan DM, Miletich JP, Zee RY, Ridker PM. Novel association of HK1 with glycated hemoglobin in a non-diabetic population: a genome-wide evaluation of 14,618 participants in the women's genome health study. *PLoS Genet* 2008;4(12):e1000312
- 35 Pastorino J, Hoek J. Regulation of hexokinase binding to VDAC. *J Bioenerg Biomembr* 2008;40(3):171–182
- 36 Allende JE, Allende CC. Protein Kinases.4. Protein-kinase CK2 – an Enzyme With Multiple Substrates and a Puzzling Regulation. *FASEB J* 1995;9(5):313–323
- 37 Tripodi F, Zinzalla V, Vanoni M, Alberghina L, Coccetti P. In CK2 inactivated cells the cyclin dependent kinase inhibitor Sic1 is involved in cell-cycle arrest before the onset of S phase. *Biochem Biophys Res Co* 2007; 359(4):921–927
- 38 Sayed M, Pelech S, Wong C, Marotta A, Salh B. Protein kinase CK2 is involved in G2 arrest and apoptosis following spindle damage in epithelial cells. *Oncogene* 2001;20(48):6994–7005
- 39 Yde CW, Olsen BB, Meek D, Watanabe N, Guerra B. The regulatory beta-subunit of protein kinase CK2 regulates cell-cycle progression at the onset of mitosis. *Oncogene* 2008;27(37):4986–4997
- 40 Wang S, Nath N, Fusaro G, Chellappan S. Rb and prohibitin target distinct regions of E2F1 for repression and respond to different upstream signals. *Mol Cell Biol* 1999;19(11):7447–7460
- 41 Sossey-Alaoui K, Kitamura E, Head K, Cowell JK. Characterization of FAM10A4, a member of the ST13 tumor suppressor gene family that maps to the 13q14.3 region associated with B-Cell leukemia, multiple myeloma, and prostate cancer. *Genomics* 2002;80(1):5–7
- 42 Bair WBI, Cabello CM, Uchida K, Bause AS, Wondrak GT. GLO1 overexpression in human malignant melanoma. *Melanoma Res* 2010;20(2): 85–96
- 43 Santarius T, Bignell GR, Greenman CD, Widaa S, Chen L, Mahoney CL, Butler A, Edkins S, Waris S, Thormalley PJ, Futreal PA, Stratton MR. GLO1-A novel amplified gene in human cancer. *Genes Chromosomes Cancer* 2010;49(8):711–725
- 44 Sakamoto H, Mashima T, Kizaki A, Dan S, Hashimoto Y, Naito M, Tsuruo T. Glyoxalase I is involved in resistance of human leukemia cells to antitumor agent-induced apoptosis. *Blood* 2000;95(10):3214–3218
- 45 Mischeau O, Tschopp J. Induction of TNF receptor I-mediated apoptosis via two sequential signaling complexes. *Cell* 2003;114(2):181–190
- 46 Toulany M, Baumann M, Rodemann HP. Stimulated PI3K-AKT signaling mediated through ligand or radiation-induced EGFR depends indirectly, but not directly, on constitutive K-Ras activity. *Mol Cancer Res* 2007;5(8):863–872
- 47 Han MJ, Wang HA, Beer LA, Tang HY, Herlyn M, Speicher DW. A systems biology analysis of metastatic melanoma using in-depth three-dimensional protein profiling. *Proteomics* 2010;10(24):4450–4462